Journal of Materials Chemistry B

Microphysiological systems for the modelling of wound healing and evaluation of pro-healing therapies

Journal:	*Journal of Materials Chemistry B*
Manuscript ID	TB-REV-02-2020-000544.R1
Article Type:	Review Article
Date Submitted by the Author:	15-Jul-2020
Complete List of Authors:	Deal, Halston; North Carolina State University and University of North Carolina, Chapel Hill, Joint Department of Biomedical Engineering Brown, Ashley; North Carolina State University College of Engineering, Biomedical Engineering Daniele, Michael; North Carolina State University, Department of Electrical and Computer Engineering; North Carolina State University and University of North Carolina, Chapel Hill, Joint Department of Biomedical Engineering

SCHOLARONE™
Manuscripts

Review

Microphysiological systems for the modeling of wound healing and evaluation of pro-healing therapies

By Halston E. Deal[1,2], Ashley C. Brown[1,2]*, and Michael A. Daniele[1,2,3]*

[1]   Joint Department of Biomedical Engineering
        North Carolina State University and University of North Carolina, Chapel Hill
        911 Oval Dr., Raleigh NC, 27695

[2]   Comparative Medicine Institute
        North Carolina State University
        1060 William Moore Dr., Raleigh, NC 27606

[3]   Department of Electrical & Computer Engineering
        North Carolina State University
        890 Oval Dr., Raleigh NC, 27695

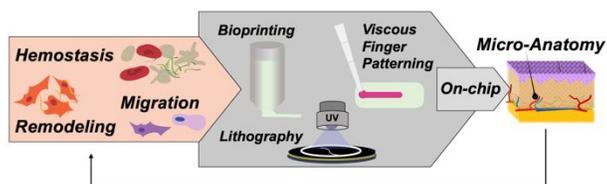[*]   Correspondence: mdaniel6@ncsu.edu; aecarso2@ncsu.edu

Table of Contents Graphic. Wound healing MPS have been engineered with synthetic and natural materials and techniques such as bioprinting or viscous finger patterning. Model designs focus on particular phases of wound healing or the recapitulation of micro-anatomies.

ABSTRACT

Wound healing is a multivariate process involving the coordinated response of numerous proteins and cell types. Accordingly, biomedical research has seen an increased adoption of the use of *in vitro* wound healing assays with complexity beyond that offered by traditional well-plate constructs. These microphysiological systems (MPS) seek to recapitulate one or more physiological features of the *in vivo* microenvironment, while retaining the analytical capacity of more reductionist assays. Design efforts to achieve relevant wound healing physiology include the use of dynamic perfusion over static culture, the incorporation of multiple cell types, the arrangement of cells in three dimensions, the addition of biomechanically and biochemically relevant hydrogels, and combinations thereof. This review provides a brief overview of the wound healing process and *in vivo* assays, and we critically review the current state of MPS and supporting technologies for modelling and studying wound healing. We distinguish between MPS that seek to inform a particular phase of wound healing, and constructs that have the potential to inform multiple phases of wound healing. This distinction is a product of whether analysis of a particular process is prioritized, or a particular physiology is prioritized, during design. Material selection is emphasized throughout, and relevant fabrication techniques discussed.

KEYWORDS

MICROPHYSIOLOGICAL SYSTEMS, WOUND HEALING, HEMOSTASIS, MIGRATION, REMODELING, MICROFLUIDICS

1. INTRODUCTION

In the United States of America, wound care is estimated to cost the healthcare system between \$28.1 and \$98.6 billion.[1] Associated efforts involve advancing therapies as well as improving laboratory models. Improvement of microphysiological modeling addresses each of these challenges, because MPS promise to facilitate therapeutic evaluation.

Wound healing is described as a combination of the cessation of extravascular blood flow, the infiltration and proliferation of inflammatory and structural cells, and the remodeling of the wounded tissue.[2-4] Some of the key cell types involved in these steps are blood cells (platelets and red blood cells [RBCs]), immune cells (macrophages, neutrophils, T cells, etc.), barrier cells (epithelial and endothelial cells), and extracellular matrix (ECM) producing cells (i.e. fibroblasts). Due to the complexity of the wound healing process, many simplified *in vitro* models have been developed to understand normal and dysfunctional wound healing processes. The etiology of dysfunctional wound healing is complex and often multifactorial, but usually involves dysregulation of one or more of the aforementioned cell types.[5] Accordingly, *in vitro* wound healing assays typically involve disrupting the function of one or more of these cell types with mechanical, thermal, electrical, optical, or chemical insult.[4, 6, 7] Traditional *in vitro* models for evaluating wound healing processes have provided much knowledge to the field, but their limited complexity leaves much room for improvement. Therefore, more complex microphysiological systems (MPS) that capture multiple aspects of the wound healing process have been the subject of development in recent years. MPS are described as *in vitro* models that recapitulate *in vivo* physiology and disease states through the anatomically relevant arrangement of 3D matrices, multiple cell types, and sometimes patient-derived cells.[8-10] Typically, wound healing implies skin as the wounded tissue, and descriptions of the remodeling phase address the remodeling of the dermis and epidermis. In this review, we discuss models of wounded skin, as well as select models of other wounded or diseased tissue, to inform the design of microphysiological systems (MPS) and their use in therapeutic evaluation, as well as the importance of material selection in designing MPS.

In general, the capacity of microphysiological systems (MPS) to inform both drug evaluation and physiology in normal and pathological states is becoming established. Increasingly, researchers are improving the microanatomical details of some *in vitro* assays and devices, because the recreation of anatomically accurate structures facilitates the recreation of structure-function relationships that are indispensable for informing biology and therapy. Wound healing is one such field, which has seen the incorporation of MPS into more research. Conventional wound healing assays have involved either 2D or animal models. More recently, researchers have begun to incorporate three dimensional gels and microfluidics into *in vitro* systems, enhancing the control of some elements in a system, while simultaneously offering more physiological relevant conditions, namely, those conferred by exposing cells to fluid flow and 3D ECM.

A critical, yet often overlooked, choice in many of these MPS is that of the materials involved. The majority of MPS consist predominantly of poly(dimethylsiloxane) (PDMS) and glass, due to their ease of use and ready incorporation into established soft lithography techniques. While established materials such as these have and likely will continue to help

inform biological phenomena, the inclusion of new materials (and novel use of existing materials) will enhance research further, especially in designs where biologically relevant materials contact cells. A difficulty in designing MPS arises in finding a balance between the complexity of the features one wants to recreate, and the materials and fabrication techniques that make it easy and/or feasible to do so. In many cases, it is easier to use a material that fails to confer the biologically relevant qualities that another, more difficult-to-use material offers. This tradeoff is evident in the plethora of PDMS microdevices and was a motivating factor for one group, for example, to use an interpenetrating agarose-gelatin network in the construction of a microvasculature, which was used to study endothelium dysfunction.[11, 12] In this article, we seek to discuss additional assays with the capacity to inform wound healing, and to emphasize design choices that help recapitulate a relevant physiology.

2. FABRICATING A RELEVANT MODEL

Historically, animal models have been considered the best non-human models of wound healing, as they confer the greatest level of complexity and include the greatest amount of relevant cell types that reductionist, non-animal models exclude[13-15]; however, the financial and ethical concerns of animal studies, along with the complimentary nature of *in vivo* and *in vitro* studies, drive the support for additional *in vitro* models, the complexity of which have necessarily been increasing beyond 2D assays,[13] in order to more accurately recreate the 3D complexity offered by animal models. Despite their complexity, popular animal models, especially rodent, suffer from mechanistic disparity between humans, such as barrier development through contractile closure instead of reepithelialization.[13, 15]

Some of the most popular wound healing animal models are the incision, excision, burn, ischemia, or infection of rodent, rabbit, or pig skin, followed by observation of the change in wound area with or without the application of a therapeutic.[13, 16] More specific measurements like that of hexosamine and hydroxyproline content, DNA content, and tensile strength can also be made.[16] Hexosamine and hydroxyproline are indicators of collagen content, collagen being the most abundant ECM protein present in skin. Zebrafish are also valid wound healing models, specifically for coagulation studies, because many of the coagulation factors are genetically and structurally conserved in humans.[17]

Even acute wound healing lasts up to 30 days, and thus, wound healing studies involve tracking of variables over long periods of time, which introduces the common limitation that numerous animals are sacrificed in wound healing experiments. Wound healing studies with human volunteers have also been utilized and have included tape stripping, suction blister, abrasion, laser, dermatome, and biopsy.[3] Human subjects inherently inform therapeutic efficacy better, but limitations such as patient enrollment, variability, and non-compliance are still present.[18, 19] Even volunteer studies raise ethical issues, namely that of challenge studies.[20] Given these limitations of animal and human studies, MPS models of wound healing could fill a critical gap in current test beds for new therapies. An overview of system design considerations in wound healing MPS has been provided in Figure 1.

Support for microphysiological systems as research tools has largely been based on the accuracy with which a model recreates the anatomy of a given structure. From there, a considerable interest has developed regarding MPS capacity to inform therapeutic efficacy.[21-24] Further justification of MPS as tools, however, has come from evaluating the cellular outputs–such as gene and protein expression– in an MPS, and comparing it to preexisting data,[25-28] especially data from *in vivo* studies, because MPS seek to complement and eventually replace *in vivo* assays. The material selection for an MPS, though critical, has not been as well developed as a means of improving MPS quality far beyond the idea of transitioning away from glass and PDMS. This review will provide an overview of wound healing, describe MPS that inform particular phases of wound healing, and finally, describe MPS that have the potential to inform multiple phases of wound healing, while placing particular emphasis on material selection.

3. WOUND HEALING OVERVIEW

Though wound healing mechanisms can be explained for single cells,[29, 30] wound healing is typically recognized as the tissue-level response to physiological damage. This response is a coordinated effort between vasculature, nervous tissue, dermal tissue, and the immune system. Nervous and vascular tissue provide immediate responses to damage, followed by progressive responses of immunological and ECM-secreting cells to orchestrate inflammation and remodeling. That said, each phase of wound healing overlaps to some degree. Clotting is the only event that must be completed within minutes, whereas the immune and proliferative responses require days to weeks to complete.

The cessation of blood flow during the hemostatic phase is accomplished by endothelial or sympathetic stimulation of VSMCs to constrict a damaged vessel,[31] and the aggregation of fibrin and platelets to arrest flow in the direction of bleeding. The latter of these two events is accomplished by a myriad of enzymes that regulate the polymerization of fibrinogen into fibrin strands, amongst which platelets bind and contract in order to densify the forming thrombus.[32] Evolution of the

multiplicity of enzymes involved in thrombus formation has resulted in a rapid, tightly regulated pathway, owing to individual enzymatic function as well as feedback loops that amplify response, such as the upregulation of thrombin activation by thrombin itself. Nonetheless, errors from infection or enzyme mutation can arise. Accordingly, hemostasis assays seek to recreate hemostatic diseases, especially hemophilia.

The proliferative or migratory phase is simply defined as the period of wound healing marked by the most significant increase in cell number. For skin, the proliferation and concomitant migration of epithelial cells is one of the most important events in wound healing because it is key to reestablishing the barrier function of skin, barrier function being the primary function of skin. Macrophages also proliferate significantly, even becoming the most numerous cell type in the average acute wound. Neutrophils and macrophages arrive from blood to regulate the inflammatory response along with resident mast cells.[2] Fibroblast migration and proliferation into the wound area is also of critical importance, particularly for facilitating the rebuilding of extracellular matrix and the subsequent remodeling phase.

Remodeling is less strictly defined than other phases of wound healing, partly because the entire process of wound healing can be considered a remodeling process of damaged tissue. More specifically, however, remodeling is the balance of ECM degradation, deposition, and organization, primarily accomplished by matrix metalloproteinases and fibroblasts.[33, 34] A critical consideration in remodeling, as well as in regenerative medicine, is that evolution has prioritized speed over resemblance.[14] In other words, formation of scar tissue is achieved prior to recapitulation of an uninjured structure and appearance. The gradual nature of remodeling is reflected in the upregulation of proteins such as osteopontin, osteonectin, CCN2, tenascin-C, and fibulin-5, which are sparse or absent in uninjured tissues.[34]

Given the complexity of each of these events in wound healing, a variety of MPS has been developed that encompass either one or more of these phases. The following sections describe traditional assays that have been used to evaluate processes in each of these stages as well as detail current developments in MPS to model important features of these wound healing stages.

4. MODELS OF WOUND HEALING

4.1 Hemostasis Assays

4.1.1 Traditional Hemostasis Assays

Common tools for assessing hemostatic events are diagnostic tools that strictly probe blood properties, rather than blood-endothelium or blood-ECM interfaces, which are also relevant in clotting. These conventional measures of hemostasis include prothrombin time (PT), activated partial thromboplastin time (aPTT), international normalized ratio (INR) and activated clotting time (ACT).[35] PT, aPTT, INR, and ACT are measures of clotting time of a patient blood sample when mixed with coagulants. Other common diagnostic techniques include thromboelastography (TEG) and rotational thromboelastography (ROTEM), each of which asses the rheological properties of blood during the progression of clotting and fibrinolysis.[36] While bulk properties like this were long considered helpful[35] in guiding surgeries and diagnoses, they are not capable of probing cellular level function.

4.1.2 MPS for Hemostasis Assays

Recent reviews have covered the utility of microvascular models on informing thrombotic[37] and blood-endothelium[38] disorders. The importance of hemostasis modeling lies primarily in the prevalence of pathological thrombosis.[37] Though the etiology of pathological thrombosis can lie in the blood itself or vessel tissue, each situation can impair or prevent wound healing. MPS promise to inform both levels of dysfunction. Many hemostatic disorders have been linked to impaired wound healing, including hemophilia.[32, 39]

One of the most complete microphysiological models of hemostasis was fabricated by Sakurai et al.[40] Their MPS consisted of three PDMS layers that allowed air pressure to move a layer in such a way that an endothelialized microchannel was "injured," by connecting a roughly 132μm wide hole to a new channel in order to simulate bleeding (Fig. 2A). The MPS allowed real-time visualization of the clotting process with the addition of whole blood mixed with corn trypsin inhibitor. Expression of phosphatidylserine (PSer) on and near the damaged endothelium was observed, and though also expressed by platelets, PSer was not surface-exposed by platelets, indicating the primary role of endothelial PSer in stimulating clotting. Sakurai et al. were also able to show that vonWillebrand Factor (vWF) primarily contributes to hemostasis at higher, arteriolar shear rates. Experiments with cell-free, collagen-coated channels were consistent with another hemostatic MPS[41]; each indicated that collagen coatings alone are not sufficient at facilitating robust clot formation, and together suggest that combinations of tissue factor, collagen, and damaged endothelial cells more sufficiently facilitate thrombus formation. Neither of these MPS were used to evaluate any therapeutics, but Schoeman et al. did simulate

Hemophilia A by blocking factor VIII with an antibody, as well as platelet aggregation dysfunction by blocking P2Y12, and ADP receptor antagonist. In the Hemophilia A simulations, platelets would aggregate but slough away from the injury vessel walls, and there was a significantly lower amount of fibrin compared to controls. Though bleeding was stopped in the P2Y12 blockage simulations in that red blood cells ceased flow through the injury channel, plasma continued to leak through, indicating a less dense thrombus than what formed in collagen-TF coating simulations.

In both of the aforementioned bleeding models,[40, 41] an extravascular space was created during or provided prior to experimentation in order to simulate mechanical vascular injury. In a previous MPS,[42] varying levels of heat were used to induce injury in HUVEC endothelium within 100x1000μm PDMS microchannels. This MPS allowed spatiotemporal control of heat application, and the spatial distribution of heat coincided with a distribution of dead endothelial cells within a channel. P-selectin and PSer distributions were also evaluated. Final platelet aggregate volumes did not show a strong correlation with shear rate; considering this, along with the variability of the role of vWF at high and low shear rates,[40] these models show that similar platelet aggregates can be achieved through non-identical mechanisms. Thrombus formation was also observed in a gelatin methacryloyl channel MPS (Fig. 2B).[43] Sacrificial channels were bio-printed with Pluronic F-127, around which the GelMA was photo-crosslinked. This MPS did not undergo any injury or wounding– clotting was induced by adding $CaCl_2$ to citrated whole blood prior to infusion. That said, the GelMA channel still provided a wound healing insight, in that GelMA-embedded fibroblasts only migrated into the clot and deposited collagen when a HUVEC endothelium was absent, suggesting that the role of fibroblasts in regulating vascular wound healing is mediated in part on the severity of endothelial damage. Endothelial inflammation was simulated with TNF-α in an endothelialized channel here.[44] This MPS was unique in that it sourced blood outgrowth endothelial cells (BOECs) from a healthy human donor, as well as from pigs and diabetic pigs. Whole blood was successfully perfused through the 75μm x 200μm (h x w) channels, and platelet aggregation could be promoted with TNF-α treatment. Thrombo-inflammatory properties were present in diabetic porcine cells without additional treatment.

4.2 Migration Assays

4.2.1 2D-based Migration Assays

Scratch wound assays have an extensive history,[45] due primarily to their ease of use, but also due to the importance of migration and associated mechanisms such as protein adhesion and cell-cell interaction the assay informs.[46] A traditional scratch wound is made by damaging or completely removing a portion of a cell sheet, often in the center of the sheet. Wound areas have been generated with pipettes, cell scrapers, metallic micro-indenters, and even toothpicks.[4] The longevity of the scratch wound assay is a testament to its informative capacity, however, difficulty in controlling cell-free areas versus cell-damage areas is present, and while many image analysis software seek to account for sample-to-sample differences,[4] microfluidic platforms offer finer control over wound area generation, while retaining much of the analytical simplicity of traditional scratch assays.

4.2.2 MPS for Migration Assays

The relative ease of use of PDMS and glass in the construction of migration assays, along with the conceptually simple construct of migration assays, has led to a relative abundance of microdevices used for migration studies. While the prevalence of migration assays may in part be due to its recognition as the limiting step of wound healing,[4] simply put, all that is needed for a migration assay is a sheet of cells, and the generation of space into which some part of that sheet can grow. An interesting distinction in the literature is that between free space without damaged cells and free space with– or juxtaposed to– damaged cells.[6, 47-49] While there is certainly value in understanding how cell sheets respond to free space alone, it is arguably more pertinent to the study of wound healing to understand how living cells respond to the presence of damaged tissue or the combination of damaged tissue and free space. Murrell et al.[6] investigated this distinction with the microfluidic design shown in Figure 3A. The three-inlet channel allowed the separate, laminar flow of cell media or trypsin, such that they could create defined regions of a denuded epithelium of mouse mammary epithelial cells. Blebbistatin, a contractility inhibitor, was also perfused over defined regions. Murrell et al. found that cell sheets migrated slower at high cell densities when a portion had been exposed to blebbistatin. This was in contrast to high-density cell sheets moving faster than low-density cell sheets after a portion had been denuded by trypsin. Interestingly, cell lysate and H_2O_2, a reactive oxygen species (ROS), each inhibited cell motility after denudation.[6] Conversely, ROS promoted Madin-Darby canine kidney epithelial migration in a previous barrier-removal study.[49] The difference in cell sheet motility, in the trypsin and blebbistatin exposures by Murrell et al., was partially regulated by the balance of tension with E-cadherin. In a "minimal tissue mimic," E-cadherin, when laterally presented to a mobile cell sheet on a silicone barrier, was sufficient at halting migration and even inducing apical-basal polarity (Fig. 4A).[50]

Other microfluidic devices have also involved the perfusion of trypsin to generate denuded areas. Wei et al.[51] fabricated a Y-shaped microchannel device housed in PDMS (Fig. 3B), that allowed perfusion of two different solutions across a cell sheet in the primary channel. Various types of VSMCs were seeded, with the intent that they inform migration tendencies relevant to atherosclerosis and intimal hyperplasia, each characterized by an increased migration tendency of VSMCs after vascular injury. Flow in these channels was achieved with gravity and no tubing was necessary. The cell types used included an established and a primary human aortic vascular smooth muscle line, a primary rat aortic vascular smooth muscle cell line, and two VSMC groups isolated from either internal mammary arteries or the ascending region of the aorta in human donors who underwent a coronary artery bypass grafting or aortic arch replacement, respectively. After denudation of cells by trypsin, migration speeds of each cell type were evaluated. Wei et al. note that while primary cell lines and cell lines should behave comparably, the human donor cells migrated much faster. The established cell line, T/G HA-VSMC, was used in chemoattractant experiments. Both TNF-α and PDGF-BB as media additions promoted faster migration than DMEM alone, and PDGF-BB promoted the fastest migration overall. Part of what makes this study significant is its evaluation of multiple different variations of the same cell type, and, accordingly, that they do not always behave similarly. This highlights the importance of such evaluations and enhances the informative power of the MPS. Lee et al.[7] used nano-patterned, fibronectin-coated PDMS ridges to study migration rate of enzymatically denuded sheets of NIH-3T3s, murine embryonic fibroblasts (Fig. 3C). Wounding experiments were performed with 1:2 ridge-to-groove width ratios, as opposed to 1:1 or 1:5, because the 1:2 patterns facilitated the greatest alignment. Unsurprisingly, the fibroblasts migrated fastest across the wound space when the nano-patterns were aligned perpendicular to the wound edges.

Another migration device consisted of removable PDMS pillars that generated circular areas into which cells could migrate (Fig. 4B).[52] Cells were simply cultured on glass and contacted some PDMS features, but the device allowed analysis of mesenchymal stem cells (MSCs) co-cultured with human gastric epithelial cells (GSE-1) or adenoid cystic carcinoma cells (ACCMs), the latter of which supported faster MSC migration. A simpler, PDMS migration device allowed manual application of pressure to generate wounds with PDMS pillars, though this leaves room for user variability of wounding pressure.[53] Circular migration regions were also generated by a device explained here.[54] This device (Fig. 4C) allowed a relatively high throughput generation of cell-free areas with limited remnants of damaged cells. The device was fabricated from off-stoichiometric thiol-ene epoxy (OSTEMER) polymer and a PDMS membrane that allowed pneumatic compression of a cell monolayer. The OSTEMER polymer can be prepared as a transparent elastomeric or rigid material.[55] Initial polymerization is achieved with UV exposure with or without a photoinitiator, and leaves the polymer solidified but flexible. Subsequent thermal curation rigidifies the material. The off-stoichiometry of the family of OSTE+ polymers allows tunability of mechanical and chemical properties, namely as surface modifications, which allow variability in wetting and binding properties.[55-57] Stoichiometric variation includes that of thiols and/or allyls. The rapid curing and low polymerization shrinkage, as well the tunability of stiffness and surface chemistries from thiol and allyl stoichiometric variation,[56] allow easy incorporation of OSTEMERs into soft lithography techniques, and the polymer has already been verified for microfluidic[57] and organ-on-chip applications.[58]

It is worth noting the popular use of TNF-α as a stimulant in many MPS, namely for its role as an inflammatory stimulant. While TNF-α has been shown to enhance VSMC migration rate relative to DMEM,[51] TNF-α has also been shown to reduce the formation of ZO-1 tight junctions in HUVECs.[59] Migration and barrier function, the latter to which ZO-1 contributes, are both critical components of wound healing, and thus TNF-α as an inflammatory cytokine has been seen with MPS to promote a more migratory phenotype, consistent with previous literature.[60, 61] That said, the promotion of migration by TNF-α is not universal according to cell type; in another study,[54] TNF-α reduced the migration rate of HUVECs.

Three dimensional gel models have been used as migration assays as well.[62] One such protocol, outlined here,[63] details the embedment of dermal fibroblast spheroids into fibrin matrices, which are indicative of early wound environments, and can be readily adapted to include other cell types, such as neutrophils and macrophages. This construct was later used to observe that synthetic platelets enhance fibroblast migration rate by contracting and stiffening fibrin clots.[64] Other examples of 3D migration models include studies in which micro-biopsies of human skin were cultured in a chip (Fig. 7A) that allowed selective neutrophil migration and analysis of their impact on *Staphylococcus aureus* growth, as well as how this could be tailored by penicillin.[65] The combination of microfluidic technology with *ex vivo* analysis is a promising way to minimize invasiveness, as the biopsies used here were generated with 23G needles. Explants also avoid the need to fabricate particular microstructures within skin, like follicles, sweat glands, or oil glands.

Thus far, the advancement of planar migration assays is primarily due to the application of microfluidic designs that enhance the accuracy of wound area generation, as well as introduce the ability to localize treatment dosage to particular

regions of cell sheets. Further advancement will likely occur with expansion and standardization of three-dimensional migration constructs. However, a challenge here is that migration through gels is much more difficult to quantify,[62] as the micro-architecture of hydrogels is more difficult to regulate than protein coatings on flat surfaces in traditional migration assays. In most 3D migration studies, cells are introduced to a 3D environment by suspension within a hydrogel or sandwiching between two hydrogels. Critical differences between migration tendencies in 2D and 3D include morphology, speed, direction, and protein expression.[62]

Another major regulator of cell phenotype is microenvironment mechanics.[66, 67] Tissue mechanics are known to depend on both extracellular material as well as cells themselves, which are recognized as major contributors to the dissipative loading behavior of tissues.[67, 68] Further, tissue culture materials like polystyrene have stiffness comparable to that of cartilage or ligament, but well above that of skin, brain, or abdominal cavity organs.[66] PDMS 184 has an elastic modulus around 2MPa[69, 70] nearer to nerve or gut,[66] but still comparable to cartilage. That said, addition of PDMS 527 to PDMS 184 can reduce elastic modulus, allowing PDMS blends to span a stiffness range from 5kPa to 1.72MPa,[69] at least in 2D, as PDMS 527 is adhesive and elastic,[71] suggesting configurations into microdevices would be more difficult.

4.3 Remodeling Assays

To our knowledge, there are no MPS specifically designed to study the remodeling phase of wound healing; instead, some wound healing assays indirectly inform remodeling. This is typically achieved with models that allow fibroblasts to operate in a 3D microenvironment.

One such MPS contained a cardiac fibroblast hydrogel channel surrounded by a PDMS device that allowed application of TGFß1 and/or cyclic strain,[72] each of which contributed to an increase in phenotypes indicative of cardiac wound healing. It is worth noting that these devices–outlined here[73]– could be deconstructed and hydrogel stiffness evaluated with a novel atomic force microscopy technique. A similar device[25] was also used to recapitulate the physiology of articular cartilage and osteoarthritis as induced by load application. This MPS is one of the most robust to date, in that physiologically relevant mechanical loads were applied, protein (types I and II collagen and aggrecan) levels and gene expression (*ACAN*, *PRG4*, *COL2A1*, *COL1A1*, *GDF5*, *ATX*, *FRZb*, and *GREM1*) were evaluated, and three different drugs (dexamethasone, rapamycin, and hyaluronic acid alkylamide 4) were all evaluated for their effect on combating inflammation and catabolism.

Another PDMS microdevice (Fig. 5A) was used to co-culture dermal fibroblasts and HUVECs with either M1 or M2 macrophages.[74] In this particular co-culture, fibroblasts differentiated to myofibroblasts independent of macrophage presence, contradictory to previous data on the effect M2 macrophages.[74] Macrophages did enhance the formation of HUVEC vessel structures, and the device was sufficient at recreating known effects of dexamethasone on IL-6 and IL-8 production. The positioning of a fibroblast monolayer and a macrophage monolayer, each alongside a 3D HUVEC-embedded gel, allowed co-culture as well as perfusion and inflammatory marker collection.

Donor fluids from acute (abdominoplasty patients) and chronic (chronic sacral decubitus) wounds were evaluated for their effect on the integrity of collagen-fibroblast gels topped with keratinocytes.[75] While control and acute wound fluid (AWF) conditions facilitated a slight increase in fibroblast count, the chronic wound fluid (CWF) completely wiped out the fibroblasts by the tenth day of culture and even degraded the collagen matrix. Comparatively, the CWF strongly increased the number of keratinocytes (Fig. 5B). AWF induced a lesser, steadier keratinocyte proliferation, and did not collapse the collagen matrix, indicative of the balance of degradation and deposition mechanisms in acute wound healing.[75] Chronic wound characteristics were also recreated in 3D collagen or fibrin gels with seeding of diabetic foot ulcer fibroblasts (DFUFs), diabetic foot fibroblasts (DFFs), and non-diabetic foot fibroblasts (NFFs).[76] Both DFUFs and DFFs promoted significantly less HUVEC sprouting in fibrin gels than NFFs, though DFFs promoted slightly more than DFUFs. DFUFs and DFFs produced less ECM and facilitated slower *in vivo* murine wound closure than NFFs as well. Interestingly, DFFs and NFFs promoted equivalent re-epithelialization rates, both significantly higher than that promoted by DFUFs. Thusly, phenotypic variability was witnessed according to cell source site as well as patient. This variability highlights the importance of considering cell source during MPS design. In another assay, excretions/secretions (ES) from *Lucilia sericata*, maggots used in chronic wound debridement, were applied to fibroblast gels of collagen and fibronectin, and found to influence the migration and contractile crosstalk between fibroblasts in a dose-dependent manner.[77] These assays demonstrate how cellular crosstalk is facilitated by three-dimensional design.

5. ANATOMY-DRIVEN MODELING APPROACHES

Until now, we have primarily discussed MPS assays with explicit indication of which phase of wound healing each is intended to model. Table 1 summarizes the cellular and material composition of these assays. The design of most of the

aforementioned models can be described as process-driven, meaning the device incorporates structures and cell types that facilitate the analysis of a particular event, e.g. cell migration, rather than recreate a particular structure or structures with which certain events can be modeled. This distinction between process-driven design and structure-driven design is similar to that of bottom-up and top-down design. The following section addresses constructs that have some capacity to inform multiple phases of wound healing, or are models of relevant anatomies, such as skin or blood vessels. Other design approaches, such as the inclusion of *ex vivo* materials, and fabrication techniques like bioprinting, are discussed. This section is not meant to be an exhaustive review of skin equivalents or *in vitro* blood vessel fabrication; rather, this section is intended to function as an overview of particular models and fabrication techniques. Recent reviews of skin constructs[78-80] have described design trends such as the movement from 2D to 3D models, use of natural polymers from ECM, and use of synthetic polymers like polylactic acid, polyethylene glycol (PEG), polyglycolic acid, polylactic-co-glycolic acid, polyhydroxybutyrate, polyvinyl alcohols, silicones, or polyurethanes. Briefly, synthetic polymers help prevent batch variability, namely in mechanical properties, while natural polymers offer superior biochemical profiles. Other efforts in skin construct design are to include appendages like hair follicles and sweat glands, as well as specialized cell types derived from iPSCs.

5.1 Hydrogels & Bioprinting

Bioprinting of hydrogels is a viable approach to *in vivo* therapy as well as *in vitro* microphysiological modeling (Fig. 7B).[81] The incorporation of a hydrogel into an MPS usually confers the benefit of studying a system in three dimensions, or at the very least, providing a near-to-fully homogenous biochemical and biomechanical microenvironment for cells. There are a handful of associated MPS fabrication methods when hydrogels are used, including pipetting, bioprinting, hydrodynamic focusing, viscous finger patterning.

Decellularized ECM (dECM), as opposed to more purified ECM, has been considered the optimal ECM type for bioink formulation.[82] Decellularization approaches include chemical, biological, and physical techniques such as acid-base treatment, detergents, enzymes, pressure and temperature changes, and mechanical agitation, each of which can help remove cells, but can damage the remaining ECM. Protocols typically involve combinations of treatments, such as in the preparation of a porcine skin dECM with freeze-thawing, shaking, trypsin, ethanol, Triton X-100, and peracetic acid,[83] or use of centrifugation, SDS, isopropanol, peracetic acid, and ethanol in the preparation of an adipose dECM.[84]

One such use of bioink dECM in an MPS is that of brain decellularized ECM (BdECM) bioink in a bio-printed brain tumor model.[85] Here, Yi et al. demonstrated the superiority of BdECM over collagen in recapitulating characteristics of glioblastoma. BdECM enhanced the proliferation of GBM cells, which also exhibited more pseudopalisading, and expressed more pro-angiogenic and ECM-remodeling genes in BdECM gel than in collagen gel. The arrangement of a surrounding stroma, consisting of HUVECs and BdECM, also enhanced the tumorigenicity of the model by establishing an oxygen gradient. Finally, this model was used to evaluate the effects of drug combinations on models with cells derived from different glioblastoma patients, and patient specificity of drug efficacy was observed. This model was effective in demonstrating not only the importance of anatomical arrangement, but the significance of material selection and patient-specific therapeutic efficacy as well. dECM from porcine small intestine supported the growth of human gastric, liver duct, fetal hepatocyte, small intestine, fetal small intestine, and fetal pancreatic organoids, as well as mouse small intestine organoids, all endodermal in origin.[86] Growth of mouse and human intestinal organoids in a laminin-fibrin gel has been outline here.[87] Recently, a bioink derived from porcine dermis has been developed and shown to support the growth of human dermal fibroblasts in 3D gels.[88, 89] This gel conferred bioactivity from collagen, growth factors, elastin, and glycosaminoglycan content. A process for preparing cartilage, adipose, and heart dECM bioinks has been outlined here.[84] The dECM gels produced by Pati et al. enhanced cellular viability and upregulation of lineage markers compared to collagen gels. A synthetic dermal gel consisting of RADA16, a peptide with a repeating arginine, aspartic acid, and alanine sequence, was used to culture keratinocytes and embedded fibroblasts for up to five weeks.[90] While this is relatively extensive, dECM gels more faithfully recapitulate tissue microenvironments due to their heterogeneous content of protein and GAGs. Further trends, techniques, and applications of skin bioprinting have been outlined here.[91, 92] It should be noted that although animal-derived dECM may be the superior choice for *in vitro* modeling, it has not been considered proper for use in humans.[93, 94] That said, decellularized human cadaver skin has recently shown comparable mechanical properties to the skin pre-decellularization,[95] making it competitive with the mechanical selectivity offered by synthetic polymers.

Blood vessels are one of the most critical anatomical structures in wound healing. Accordingly, we have included some blood vessel models and fabrication techniques that have the potential to improve our understanding of wound healing physiology, as well as enhance design considerations in wound healing MPS design. In one study,[96] a custom device was used to support the perfusion of a collagen-based, endothelialized tissue engineered blood vessel (TEBV) – fabricated by

compression around a mandrel– for up to 5 weeks. This relatively extensive perfusability carries potential for chronic wound healing studies, as there is a current lack of MPS that model a chronic wound, and robust experimentation with such a device would need to last approximately three months– this said, an exact timeline for chronicity is not universal.[97] Hasan et al. outlined a technique for the fabrication of a tri-layer blood vessel-like structure housed in PDMS.[98] This fabrication technique is significant in that it involves the production of more than two vessel layers. The lumen of these vessels supported the growth of HUVECs, which were surrounded by SMCs and fibroblasts in outer layers.

Another technique used in blood vessel MPS fabrication is viscous patterning, which takes advantage of the process of viscous fingering (Fig. 6). Viscous fingering is the movement of a less viscous fluid through a more viscous one, and was first taken advantage of in the on-chip fabrication of hydrogel lumen here,[99] and expanded in devices that facilitate angiogenesis from a parent vessel.[100] This process was later used to generate cellularized TEBVs with human induced pluripotent stem cells (hiPSCs).[101] hiPSC differentiation into endothelial cells make this TEBV design a promising construct for personalized drug evaluation.[101] More complicated viscous patterning principles, involving the control of branching patterns, have been outlined here.[102] Another unique approach to vessel formation also takes advantage of fluidic principles; core-sheath flow by hydrodynamic focusing is the alignment of concentric layers of flowing fluids. Cell-laden gels can be aligned and polymerized upon or prior to extrusion from a flow-alignment vessel. One group crosslinked alginate fibers with $CaCl_2$ and incorporated these fibers into a blood-brain barrier chip.[103] Another group has photo-crosslinked PEG-GelMA hydrogel fibers, which underwent angiogenesis in both Matrigel and GelMA.[104] Additional devices for producing cell-encapsulated fibers have been reviewed here.[105]

Further promise for investigating vessel dysfunction, specifically endothelial cell dysfunction, was shown by Qiu et al. with an interpenetrating network of agarose and gelatin.[11] While this device has glass and PDMS casing for microscopy, the channels in which the cells reside consist entirely of the agarose-gelatin IPN, thus, the endothelium witnessed a stiffness similar to actual vasculature at about 25kPa. The vessel model allowed the establishment of endothelial barrier function, which was reduced and restored upon the introduction and removal of either TNF-α, sickle cells, or *Plasmodium*-infected RBCs. The microvasculature model was sustained for over a month at a time, making it another significant step towards *in vitro* modeling of chronic vessel conditions.

5.2 Explants & Human Skin Equivalents

Another approach to material selection, rather than synthesize a new material or modify a biological material, is the incorporation of developed tissue into MPS. Incorporation of explants as well as tissues developed in vascularized chambers[106] could eliminate the need to "construct" recapitulative tissues; if something has been grown *in vivo*, it would not recapitulate, but innately have a given physiology. Thus far, vascularized chambers have already been used to develop adipose, skeletal myoblast, cardiac, liver, thymus, pancreatic, breast, and pituitary tissue.[106] A drawback to this technique is the surgical skill required, contributing to the motivation for collaborative, interdisciplinary research. Also, the need to grow the chambers within an animal would detract from the animal-free, reduced-cost, high-throughput benefits of using MPS for drug evaluation. That said, vascularized chambers (Fig. 7C) have already been established in mice, rats, rabbits, sheep, pigs, and even humans.[106] To our knowledge, vascularized chambers have not been used for the development of any MPS.

Human skin equivalents (HSEs) have been fabricated in an effort to subject cells to a spatial composition more similar to that found *in vivo* than in simple monolayer assays. In one such HSE model, fibroblasts were cultured in a collagen I matrix and keratinocytes grown and cornified on the gel at an air-liquid interface.[107] The gel was housed in a 3mm tall, 6mm diameter hole in PDMS, which was separated from a PDMS microchannel for media perfusion by a polycarbonate membrane. Long-term (up to 4 weeks of keratinocyte proliferation) maintenance of a skin equivalent was performed, and doxorubicin treatment was shown to disrupt the epidermal-dermal interface. Dermal fibroblasts and HaCaT keratinocytes were cultured in and on, respectively, another collagen hydrogel, which was house in a PDMS microfluidic device that allowed perfusion into the dermal-epidermal construct by alternative rocking of the device.[108] The authors point out the irregular epidermal structure compared to static transwell culture, and suggest this may be due to the irregular transportation patterns of nutrients due to the rocking; accordingly, they identify the need for vascular structures in skin equivalents and suggest that this can not only enhance nutrient transport in skin equivalents, but allow for the introduction of immune cells like neutrophils, during wound healing experiments. Despite a significant reduction in cell viability between 5 and 10 days, this MPS still demonstrated the significance of dynamic culture in enhancing cell viability. Another group prolonged the culture of EpiDermFT™ (Mattek, Ashland, MA, USA) skin equivalents with a dynamic culture "Multi-Organ-Chip" (MOC), which they also showed was superior in maintaining *ex vivo* juvenile prepuce skin biopsies (Fig. 7A), and sustained pilosebaceous unit explants for two weeks.[109] The same MOC was used to co-culture liver microtissue and skin biopsies, which underwent metabolic crosstalk per albumin production and consumption[110]; the liver microtissue experienced a

cytochrome P450 3A4 dose-dependency to troglitazone, demonstrating the usability of the liver-skin MPS in drug evaluation experiments. Hair follicle skin constructs were created by casting collagen gels around 3D-printed column molds with high aspect ratios (4mm length and 500μm diameter).[111] Gel wells were subsequently seeded with dermal papilla cell (DPC) spheroids and keratinocytes. Sparse hair growth was witnessed *in vitro*, and *Lef-1* gene upregulation and encapsulation of HUVECs into the gel enhanced the follicular units' propensity to grow human hair in mice. Hair growth from a collagen gel is significant, and largely attributable to the vascular support by HUVECs, performance of DPCs over regular dermal fibroblasts, and upregulation of *Lef-1*; however, the success of dECM gels in directing cell phenotype, promises to improve functional characteristics of such follicular units even further. Efforts to add functionality to skin equivalents has also been pursued with melanocyte addition. In one construct, fibroblasts, keratinocytes, and melanocytes were all derived from iPSCs and added to a collagen I gel. Melanocytes localized to the basal region of the epidermis and produced melanosomes that were taken up by keratinocytes.[112]

One of the most robust skin constructs was a bioink fabricated by Kim et al.[113] Their bioink was a porcine skin-derived ECM (S-dECM), and it contained a heterogenous mixture of ECM components more indicative of native skin than collagen bioinks: collagen, GAGs, elastin, hyaluronic acid (HA). *In vitro* experiments revealed increased mRNA expression for collagens I and III, fibronectin, decorin, vimentin, and KGF-1, along with >90% cell viability at 7 days of culture, despite being static culture. The quality of this S-dECM was further demonstrated by its lesser shrinkage, which facilitated superior neovascularization and re-epithelialization in *in vivo* murine wounds. A bioprinting process[89] outlined by Ahn et al. describes the benefit of uniform thermal crosslinking of porcine-derived dECM bioink during printing for achieving stable structures. Importantly, bioink source tissues vary in concentration of collagen, elastin, GAGs, etc., and thus bioprinting parameters for dECM bioinks are difficult to universalize.[89, 113] Another limitation in extrusion-based bioprinting is the tradeoff between stability conferred by larger prints, and necessary nutrient diffusion rates conferred by smaller prints.[114] Though laser-based bioprinting (LBB) and droplet-based bioprinting (DBB) offer finer control over small resolution prints, LBB suffers from higher instrumentation costs and potential biocompatibility issues from metal films and crosslinkers; DBB is much less compatible with higher viscosity bioinks.[114]

dECM may be the most promising material choice for functional hydrogels, however semisynthetic options (Fig. 7D, E) like the poly(ethylene glycol)-gelatin gel developed by Klotz et al.[115] remain competitive due to its facilitation of the growth of vessel-like structures and the growth of bone-like and liver-like tissues better than Matrigel.

Histology, immunofluorescence, and PCR are each valid methods for evaluating HSEs, but Confocal Raman Spectroscopy (RCS) offers a non-invasive way to measure thickness and avoid artifacts from chemical fixation.[116] Transepithelial electrical resistance (TEER) also avoids fixation and has been validated as a measure of skin construct barrier strength.[117] Due largely to its high print speed, a new light-based approach[118] may become superior to previous approaches for bioprinting of skin constructs. Cell-laden GelMA constructs could be printed within ten seconds and maintain viability above 85%. This technology utilizes a Radon transform to project a collection of 2D patterns into a rotating gel chamber, as inspired by optical tomography.

6. CONCLUDING REMARKS

A major barrier in the efficacy of many microphysiological systems in informing biology and therapy is the lack of immune-competency. Wound healing is a multi-week process and immune cells are involved virtually the entire time.[2] Neutrophils and macrophages alone are the most abundant cell types during wound healing,[2] yet keratinocytes and fibroblasts are the most prevalent cell type in *in vitro* wound healing and skin disease assays.[13, 119] In order for wound healing models, or models of any physiological process to become more effective, more researchers will need to start including immune cells along with the more popular epithelial, endothelial, and fibroblastic cells characteristic of *in vitro* wound healing assays. One option for immune cell incorporation is that of neutrophils into hemostasis or migration assays, as platelets are known to attract neutrophils with IL-8.[120] Devices that facilitate the damage of cells, such as those in Figures 4B and 4C, stand to benefit from macrophage incorporation, as macrophages are known to phagocytose cell debris.[120] Further improvements to MPS design will be made with mathematical modeling and consideration of allometric relations between humans and MPS[121]– allometric relations describe the relations between organism size and a physiological parameter such as metabolic rate.

Animal and human volunteer models are still the most informative for the macro-physiology of wound healing and the efficacy of therapeutics, and MPS need to become more complex, or offer truly unique information with reductionist approaches, in order to match the informative capacity of *in vivo* models. One of the primary ways in which they will become more informative is with the inclusion of multiple physiologically relevant features simultaneously, with reduced

sacrifice of relevant mechanical, biochemical, and anatomical conditions. This said, there is still plenty to learn from reductionist devices, such as the single-cell guillotine[29] that allows rapid splitting of multiple cells, sequentially– even single-cell wounding has the potential to inform multicellular wound healing mechanisms.[30] A significant limitation to human studies is that chronic wounding could never be induced in a challenge study. Chronic wounds are the most common type of pathological wound seen clinically,[122] and associated treatment costs total many billions of dollars annually.[1, 123] The motivation to produce wound models that can be sustained for extensive periods in order to accurately recapitulate chronic conditions, as well as evaluate therapeutic efficacy is three-fold: ethical, medical, and financial.

Wound healing MPS and HSCs will be improved by incorporating dECM, iPSCs, dynamic culture, immune cells, and combinations thereof. Laboratories with skill in incorporating each of these features into a given device are limited, however, and thus, the challenge of improving MPS is rooted in interdisciplinary efforts. We do not explicitly discourage the use of PDMS or homogenous hydrogels, as these materials can still be valuable for traditional experimentation, validations, or proof-of-concepts. Nonetheless, as wound healing MPS become more sophisticated and readily available, they will certainly become a critical experimental and diagnostic tool for wound healing research.

ACKNOWLEDGEMENTS

REFERENCES

1.   C. K. Sen, *Adv Wound Care (New Rochelle)*, 2019, **8**, 39-48.
2.   L. Canedo-Dorantes and M. Canedo-Ayala, *Int J Inflam*, 2019, **2019**, 3706315.
3.   K. P. Wilhelm, D. Wilhelm and S. Bielfeldt, *Skin Res Technol*, 2017, **23**, 3-12.
4.   A. Stamm, K. Reimers, S. Strauß, P. Vogt, T. Scheper and I. Pepelanova, *BioNanoMaterials*, 2016, **17**.
5.   T. N. Demidova-Rice, M. R. Hamblin and I. M. Herman, *Adv Skin Wound Care*, 2012, **25**, 304-314.
6.   M. Murrell, R. Kamm and P. Matsudaira, *PLoS One*, 2011, **6**, e24283.
7.   I. Lee, D. Kim, G. L. Park, T. J. Jeon and S. M. Kim, *PLoS One*, 2018, **13**, e0201418.
8.   G. A. Truskey, *Front Public Health*, 2018, **6**, 185.
9.   L. A. Low and D. A. Tagle, *Lab Chip*, 2017, **17**, 3026-3036.
10.   C. D. Edington, W. L. K. Chen, E. Geishecker, T. Kassis, L. R. Soenksen, B. M. Bhushan, D. Freake, J. Kirschner, C. Maass, N. Tsamandouras, J. Valdez, C. D. Cook, T. Parent, S. Snyder, J. Yu, E. Suter, M. Shockley, J. Velazquez, J. J. Velazquez, L. Stockdale, J. P. Papps, I. Lee, N. Vann, M. Gamboa, M. E. LaBarge, Z. Zhong, X. Wang, L. A. Boyer, D. A. Lauffenburger, R. L. Carrier, C. Communal, S. R. Tannenbaum, C. L. Stokes, D. J. Hughes, G. Rohatgi, D. L. Trumper, M. Cirit and L. G. Griffith, *Sci Rep*, 2018, **8**, 4530.
11.   Y. Qiu, B. Ahn, Y. Sakurai, C. E. Hansen, R. Tran, P. N. Mimche, R. G. Mannino, J. C. Ciciliano, T. J. Lamb, C. H. Joiner, S. F. Ofori-Acquah and W. A. Lam, *Nat Biomed Eng*, 2018, **2**, 453-463.
12.   J. Motherwell and W. L. Murfee, *Nature Biomedical Engineering*, 2018, **2**, 349-350.
13.   D. G. Sami, H. H. Heiba and A. Abdellatif, *Wound Medicine*, 2019, **24**, 8-17.
14.   D. M. Ansell, K. A. Holden and M. J. Hardman, *Exp Dermatol*, 2012, **21**, 581-585.
15.   R. Perez and S. C. Davis, *Wounds*, 2008, **20**, 3-8.
16.   A. Shrivastav, A. K. Mishra, S. S. Ali, A. Ahmad, M. F. Abuzinadah and N. A. Khan, *Wound Medicine*, 2018, **20**, 43-53.
17.   A. C. Weyand and J. A. Shavit, *Curr Opin Hematol*, 2014, **21**, 418-422.
18.   S. Cullati, D. S. Courvoisier, A. Gayet-Ageron, G. Haller, O. Irion, T. Agoritsas, S. Rudaz and T. V. Perneger, *BMC Med Res Methodol*, 2016, **16**, 50.
19.   A. H. Morris and J. P. A. Ioannidis, *Chest*, 2013, **143**, 1127-1135.
20.   T. Hope and J. McMillan, *J Med Ethics*, 2004, **30**, 110-116.
21.   L. A. Low and D. A. Tagle, *Clin Transl Sci*, 2017, **10**, 237-239.
22.   N. Isoherranen, R. Madabushi and S. M. Huang, *Clin Transl Sci*, 2019, **12**, 113-121.
23.   L. Ewart, E. Dehne, K. Fabre, S. Gibbs, J. Hickman, E. Hornberg, M. Ingelman-Sundberg, K. Jang, D. R. Jones, V. M. Lauschke, U. Marx, J. T. Mettetal, A. Pointon, D. Williams, W. Zimmermann and P. Newham, *Annual Review of Pharmacology and Toxicology*, 2017, **58**, 65–82.
24.   E.-M. Dehne, A. Winter and U. Marx, *Current Opinion in Toxicology*, 2019, **17**, 18-22.
25.   P. Occhetta, A. Mainardi, E. Votta, Q. Vallmajo-Martin, M. Ehrbar, I. Martin, A. Barbero and M. Rasponi, *Nat Biomed Eng*, 2019, **3**, 545-557.
26.   S. Jalili-Firoozinezhad, F. S. Gazzaniga, E. L. Calamari, D. M. Camacho, C. W. Fadel, A. Bein, B. Swenor, B. Nestor, M. J. Cronce, A. Tovaglieri, O. Levy, K. E. Gregory, D. T. Breault, J. M. S. Cabral, D. L. Kasper, R. Novak and D. E. Ingber, *Nat Biomed Eng*, 2019, **3**, 520-531.
27.   S. Musah, A. Mammoto, T. C. Ferrante, S. S. F. Jeanty, M. Hirano-Kobayashi, T. Mammoto, K. Roberts, S. Chung, R. Novak, M. Ingram, T. Fatanat-Didar, S. Koshy, J. C. Weaver, G. M. Church and D. E. Ingber, *Nat Biomed Eng*, 2017, **1**.
28.   O. Kilic, A. Yoon, S. R. Shah, H. M. Yong, A. Ruiz-Valls, H. Chang, R. A. Panettieri, Jr., S. B. Liggett, A. Quinones-Hinojosa, S. S. An and A. Levchenko, *Nat Biomed Eng*, 2019, **3**, 532-544.
29.   L. R. Blauch, Y. Gai, J. W. Khor, P. Sood, W. F. Marshall and S. K. Y. Tang, *Proc Natl Acad Sci U S A*, 2017, **114**, 7283-7288.

30.   M. T. Abreu-Blanco, J. M. Verboon and S. M. Parkhurst, *Bioarchitecture*, 2011, **1**, 114-121.

31.   P. Teller and T. K. White, *Perioperative Nursing Clinics*, 2011, **6**, 159-170.

32.   H. H. Versteeg, J. W. Heemskerk, M. Levi and P. H. Reitsma, *Physiol Rev*, 2013, **93**, 327-358.

33.   S. Singh, A. Young and C.-E. McNaught, *Surgery (Oxford)*, 2017, **35**, 473-477.

34.   L. E. Tracy, R. A. Minasian and E. J. Caterson, *Adv Wound Care (New Rochelle)*, 2016, **5**, 119-136.

35.   J. H. Levy, F. Szlam, A. S. Wolberg and A. Wrinkler, *Clinics in Laboratory Medicine*, 2014, **34**, 453–457.

36.   H. T. Peng, B. Nascimento and A. Beckett, *Biomed Res Int*, 2018, **2018**, 7020539.

37.   N. K. R. Pandian, R. G. Mannino, W. A. Lam and A. Jain, *Current Opinion in Biomedical Engineering*, 2018, **5**, 29-34.

38.   C. A. Hesh, Y. Qiu and W. A. Lam, *Micromachines (Basel)*, 2019, **11**.

39.   M. Hoffman, A. Harger, A. Lenkowski, U. Hedner, H. R. Roberts and D. M. Monroe, *Blood*, 2006, **108**, 3053-3060.

40.   Y. Sakurai, E. T. Hardy, B. Ahn, R. Tran, M. E. Fay, J. C. Ciciliano, R. G. Mannino, D. R. Myers, Y. Qiu, M. A. Carden, W. H. Baldwin, S. L. Meeks, G. E. Gilbert, S. M. Jobe and W. A. Lam, *Nat Commun*, 2018, **9**, 509.

41.   R. M. Schoeman, K. Rana, N. Danes, M. Lehmann, J. A. Di Paola, A. L. Fogelson, K. Leiderman and K. B. Neeves, *Cell Mol Bioeng*, 2017, **10**, 3-15.

42.   J. L. Sylman, D. T. Artzer, K. Rana and K. B. Neeves, *Integr Biol (Camb)*, 2015, **7**, 801-814.

43.   Y. S. Zhang, F. Davoudi, P. Walch, A. Manbachi, X. Luo, V. Dell'Erba, A. K. Miri, H. Albadawi, A. Arneri, X. Li, X. Wang, M. R. Dokmeci, A. Khademhosseini and R. Oklu, *Lab Chip*, 2016, **16**, 4097-4105.

44.   T. Mathur, K. A. Singh, R. P. NK, S. H. Tsai, T. W. Hein, A. K. Gaharwar, J. M. Flanagan and A. Jain, *Lab Chip*, 2019, **19**, 2500-2511.

45.   G. J. Todaro, G. K. Lazar and H. Green, *Journal of Cellular Physiology*, 1965, **66**, 325–333.

46.   C. C. Liang, A. Y. Park and J. L. Guan, *Nat Protoc*, 2007, **2**, 329-333.

47.   R. van Horssen, N. Galjart, J. A. Rens, A. M. Eggermont and T. L. ten Hagen, *J Cell Biochem*, 2006, **99**, 1536-1552.

48.   M. Poujade, E. Grasland-Mongrain, A. Hertzog, J. Jouanneau, P. Chavrier, B. Ladoux, A. Buguin and P. Silberzan, *Proc Natl Acad Sci U S A*, 2007, **104**, 15988-15993.

49.   D. L. Nikolic, A. N. Boettiger, D. Bar-Sagi, J. D. Carbeck and S. Y. Shvartsman, *Am J Physiol Cell Physiol*, 2006, **291**, C68-75.

50.   D. J. Cohen, M. Gloerich and W. J. Nelson, *Proc Natl Acad Sci U S A*, 2016, **113**, 14698-14703.

51.   Y. Wei, F. Chen, T. Zhang, D. Chen, X. Jia, J. Wang, W. Guo and J. Chen, *Sci Rep*, 2015, **5**, 14049.

52.   M. Zhang, H. Li, H. Ma and J. Qin, *Wound Repair Regen*, 2013, **21**, 897-903.

53.   H. Go, T. Tian and S. W. Rhee, *BioChip Journal*, 2018, **12**, 146-153.

54.   D. Sticker, S. Lechner, C. Jungreuthmayer, J. Zanghellini and P. Ertl, *Anal Chem*, 2017, **89**, 2326-2333.

55.   F. Saharil, F. Forsberg, Y. Liu, P. Bettotti, N. Kumar, F. Niklaus, T. Haraldsson, W. van der Wijngaart and K. B. Gylfason, *Journal of Micromechanics and Microengineering*, 2013, **23**.

56.   C. F. Carlborg, T. Haraldsson, K. Oberg, M. Malkoch and W. van der Wijngaart, *Lab Chip*, 2011, **11**, 3136-3147.

57.   N. Sandström, R. Z. Shafagh, A. Vastesson, C. F. Carlborg, W. van der Wijngaart and T. Haraldsson, *Journal of Micromechanics and Microengineering*, 2015, **25**.

58.   D. Sticker, M. Rothbauer, S. Lechner, M. T. Hehenberger and P. Ertl, *Lab Chip*, 2015, **15**, 4542-4554.

59.   M. Wufuer, G. Lee, W. Hur, B. Jeon, B. J. Kim, T. H. Choi and S. Lee, *Sci Rep*, 2016, **6**, 37471.

60.   R. Montesano, P. Soulie, J. A. Eble and F. Carrozzino, *J Cell Sci*, 2005, **118**, 3487-3500.

61.   R. C. Bates and A. M. Mercurio, *Molecular Bilogy of the Cell*, 2003, **14**, 1790–1800.

62.   L. T. Vu, G. Jain, B. D. Veres and P. Rajagopalan, *Tissue Eng Part B Rev*, 2015, **21**, 67-74.

63.   S. Nandi and A. C. Brown, *J Vis Exp*, 2017, DOI: 10.3791/56099.

64. S. Nandi, E. P. Sproul, K. Nellenbach, M. Erb, L. Gaffney, D. O. Freytes and A. C. Brown, *Biomater Sci*, 2019, **7**, 669-682.

65. J. J. Kim, F. Ellett, C. N. Thomas, F. Jalali, R. R. Anderson, D. Irimia and A. B. Raff, *Lab Chip*, 2019, **19**, 3094-3103.

66. C. F. Guimarães, L. Gasperini, A. P. Marques and R. L. Reis, *Nature Reviews Materials*, 2020, **5**, 351-370.

67. A. E. Miller, P. Hu and T. H. Barker, *Adv Healthc Mater*, 2020, **9**, e1901445.

68. K. A. Marx, T. Zhou, A. Montrone, D. McIntosh and S. J. Braunhut, *Anal Biochem*, 2005, **343**, 23-34.

69. R. N. Palchesko, L. Zhang, Y. Sun and A. W. Feinberg, *PLoS One*, 2012, **7**, e51499.

70. Z. Wang, A. A. Volinsky and N. D. Gallant, *Journal of Applied Polymer Science*, 2014, **131**, n/a-n/a.

71. N. Abdul, Masters Masters, University of New Mexico, 2016.

72. P. Occhetta, G. Isu, M. Lemme, C. Conficconi, P. Oertle, C. Räz, R. Visone, G. Cerino, M. Plodinec, M. Rasponi and A. Marsano, *Integrative Biology*, 2018, **10**, 174-183.

73. A. Marsano, C. Conficconi, M. Lemme, P. Occhetta, E. Gaudiello, E. Votta, G. Cerino, A. Redaelli and M. Rasponi, *Lab Chip*, 2016, **16**, 599-610.

74. S. Biglari, T. Y. L. Le, R. P. Tan, S. G. Wise, A. Zambon, G. Codolo, M. De Bernard, M. Warkiani, A. Schindeler, S. Naficy, P. Valtchev, A. Khademhosseini and F. Dehghani, *Adv Healthc Mater*, 2019, **8**, e1801307.

75. B. Manuela, K. Milad, S. Anna-Lena, R. Julian-Dario, S. Ewa Klara and L. Ye, *Journal of Tissue Repair and Regeneration*, 2017, **1**, 1-11.

76. A. G. Maione, Y. Brudno, O. Stojadinovic, L. K. Park, A. Smith, A. Tellechea, E. C. Leal, C. J. Kearney, A. Veves, M. Tomic-Canic, D. J. Mooney and J. A. Garlick, *Tissue Eng Part C Methods*, 2015, **21**, 499-508.

77. A. J. Horobin, K. M. Shakesheff and D. I. Pritchard, *J Invest Dermatol*, 2006, **126**, 1410-1418.

78. M. J. Randall, A. Jungel, M. Rimann and K. Wuertz-Kozak, *Front Bioeng Biotechnol*, 2018, **6**, 154.

79. A. K. Dabrowska, G. M. Rotaru, S. Derler, F. Spano, M. Camenzind, S. Annaheim, R. Stampfli, M. Schmid and R. M. Rossi, *Skin Res Technol*, 2016, **22**, 3-14.

80. H. E. Abaci, Z. Guo, Y. Doucet, J. Jackow and A. Christiano, *Exp Biol Med (Maywood)*, 2017, **242**, 1657-1668.

81. P. He, J. Zhao, J. Zhang, B. Li, Z. Gou, M. Gou and X. Li, *Burns Trauma*, 2018, **6**, 5.

82. F. Kabirian and M. Mozafari, *Methods*, 2019, DOI: 10.1016/j.ymeth.2019.04.019.

83. M. T. Wolf, K. A. Daly, E. P. Brennan-Pierce, S. A. Johnson, C. A. Carruthers, A. D'Amore, S. P. Nagarkar, S. S. Velankar and S. F. Badylak, *Biomaterials*, 2012, **33**, 7028-7038.

84. F. Pati, J. Jang, D. H. Ha, S. Won Kim, J. W. Rhie, J. H. Shim, D. H. Kim and D. W. Cho, *Nat Commun*, 2014, **5**, 3935.

85. H. G. Yi, Y. H. Jeong, Y. Kim, Y. J. Choi, H. E. Moon, S. H. Park, K. S. Kang, M. Bae, J. Jang, H. Youn, S. H. Paek and D. W. Cho, *Nat Biomed Eng*, 2019, **3**, 509-519.

86. G. G. Giobbe, C. Crowley, C. Luni, S. Campinoti, M. Khedr, K. Kretzschmar, M. M. De Santis, E. Zambaiti, F. Michielin, L. Meran, Q. Hu, G. van Son, L. Urbani, A. Manfredi, M. Giomo, S. Eaton, D. Cacchiarelli, V. S. W. Li, H. Clevers, P. Bonfanti, N. Elvassore and P. De Coppi, *Nat Commun*, 2019, **10**, 5658.

87. N. Broguiere, L. Isenmann, C. Hirt, T. Ringel, S. Placzek, E. Cavalli, F. Ringnalda, L. Villiger, R. Zullig, R. Lehmann, G. Rogler, M. H. Heim, J. Schuler, M. Zenobi-Wong and G. Schwank, *Adv Mater*, 2018, **30**, e1801621.

88. J. Y. Won, M. H. Lee, M. J. Kim, K. H. Min, G. Ahn, J. S. Han, S. Jin, W. S. Yun and J. H. Shim, *Artif Cells Nanomed Biotechnol*, 2019, **47**, 644-649.

89. G. Ahn, K. H. Min, C. Kim, J. S. Lee, D. Kang, J. Y. Won, D. W. Cho, J. Y. Kim, S. Jin, W. S. Yun and J. H. Shim, *Sci Rep*, 2017, **7**, 8624.

90. B. Kao, K. Kadomatsu and Y. Hosaka, *TISSUE ENGINEERING: Part A*, 2009, **15**, 2385–2396.

91. R. Augustine, *Prog Biomater*, 2018, **7**, 77-92.

92.	S. Vijayavenkataraman, W. F. Lu and J. Y. Fuh, *Biofabrication*, 2016, **8**, 032001.
93.	M. Parmaksiz, A. Dogan, S. Odabas, A. E. Elcin and Y. M. Elcin, *Biomed Mater*, 2016, **11**, 022003.
94.	K. Dzobo, K. Motaung and A. Adesida, *Int J Mol Sci*, 2019, **20**.
95.	P. B. Milan, N. Lotfibakhshaiesh, M. T. Joghataie, J. Ai, A. Pazouki, D. L. Kaplan, S. Kargozar, N. Amini, M. R. Hamblin, M. Mozafari and A. Samadikuchaksaraei, *Acta Biomater*, 2016, **45**, 234-246.
96.	C. E. Fernandez, R. W. Yen, S. M. Perez, H. W. Bedell, T. J. Povsic, W. M. Reichert and G. A. Truskey, *Sci Rep*, 2016, **6**, 21579.
97.	S. Bernell and S. W. Howard, *Front Public Health*, 2016, **4**, 159.
98.	A. Hasan, A. Paul, A. Memic and A. Khademhosseini, *Biomed Microdevices*, 2015, **17**, 88.
99.	L. L. Bischel, S. H. Lee and D. J. Beebe, *J Lab Autom*, 2012, **17**, 96-103.
100.	L. L. Bischel, E. W. Young, B. R. Mader and D. J. Beebe, *Biomaterials*, 2013, **34**, 1471-1477.
101.	M. N. S. de Graaf, A. Cochrane, F. E. van den Hil, W. Buijsman, A. D. van der Meer, A. van den Berg, C. L. Mummery and V. V. Orlova, *APL Bioeng*, 2019, **3**, 026105.
102.	T. U. Islam and P. S. Gandhi, *Sci Rep*, 2017, **7**, 16602.
103.	T. P. T. Nguyen, B. M. Tran and N. Y. Lee, *Journal of Materials Chemistry B*, 2018, **6**, 6057-6066.
104.	K. A. DiVito, M. A. Daniele, S. A. Roberts, F. S. Ligler and A. A. Adams, *Biomaterials*, 2017, **138**, 142-152.
105.	M. A. Daniele, D. A. Boyd, A. A. Adams and F. S. Ligler, *Adv Healthc Mater*, 2015, **4**, 11-28.
106.	K. K. Yap, G. C. Yeoh, W. A. Morrison and G. M. Mitchell, *Trends Biotechnol*, 2018, **36**, 1011-1024.
107.	H. E. G. Abaci, K.; Guo, Z.; Christiano, A.M. ; Shuler, M.L., *Lab Chip*, 2015, **15**, 882–888.
108.	S. Lee, S. P. Jin, Y. K. Kim, G. Y. Sung, J. H. Chung and J. H. Sung, *Biomed Microdevices*, 2017, **19**, 22.
109.	B. Atac, I. Wagner, R. Horland, R. Lauster, U. Marx, A. G. Tonevitsky, R. P. Azar and G. Lindner, *Lab Chip*, 2013, **13**, 3555-3561.
110.	I. Wagner, E. M. Materne, S. Brincker, U. Sussbier, C. Fradrich, M. Busek, F. Sonntag, D. A. Sakharov, E. V. Trushkin, A. G. Tonevitsky, R. Lauster and U. Marx, *Lab Chip*, 2013, **13**, 3538-3547.
111.	H. E. Abaci, A. Coffman, Y. Doucet, J. Chen, J. Jackow, E. Wang, Z. Guo, J. U. Shin, C. A. Jahoda and A. M. Christiano, *Nat Commun*, 2018, **9**, 5301.
112.	K. Gledhill, Z. Guo, N. Umegaki-Arao, C. A. Higgins, M. Itoh and A. M. Christiano, *PLoS One*, 2015, **10**, e0136713.
113.	B. S. Kim, Y. W. Kwon, J. S. Kong, G. T. Park, G. Gao, W. Han, M. B. Kim, H. Lee, J. H. Kim and D. W. Cho, *Biomaterials*, 2018, **168**, 38-53.
114.	P. Sasmal, P. Datta, Y. Wu and I. T. Ozbolat, *Microphysiol Syst*, 2018, **2**.
115.	B. J. Klotz, L. A. Oosterhoff, L. Utomo, K. S. Lim, Q. Vallmajo-Martin, H. Clevers, T. B. F. Woodfield, A. Rosenberg, J. Malda, M. Ehrbar, B. Spee and D. Gawlitta, *Adv Healthc Mater*, 2019, **8**, e1900979.
116.	Y. Dancik, G. Sriram, B. Rout, Y. Zou, M. Bigliardi-Qi and P. L. Bigliardi, *Analyst*, 2018, **143**, 1065-1076.
117.	Q. Ramadan and F. C. Ting, *Lab Chip*, 2016, **16**, 1899-1908.
118.	P. N. Bernal, P. Delrot, D. Loterie, Y. Li, J. Malda, C. Moser and R. Levato, *Adv Mater*, 2019, **31**, e1904209.
119.	M. A. Frade, T. A. Andrade, A. F. Aguiar, F. A. Guedes, M. N. Leite, W. R. Passos, E. B. Coelho and P. K. Das, *An Bras Dermatol*, 2015, **90**, 347-350.
120.	S. Ellis, E. J. Lin and D. Tartar, *Curr Dermatol Rep*, 2018, **7**, 350-358.
121.	J. H. Sung, Y. Wang and M. L. Shuler, *APL Bioeng*, 2019, **3**, 021501.
122.	T. V. Boyko, M. T. Longaker and G. P. Yang, *Plast Reconstr Surg*, 2017, **139**, 654-662.
123.	S. R. Nussbaum, M. J. Carter, C. E. Fife, J. DaVanzo, R. Haught, M. Nusgart and D. Cartwright, *Value Health*, 2018, **21**, 27-32.
124.	Z. W. K. Low, Z. Li, C. Owh, P. L. Chee, E. Ye, K. Dan, S. Y. Chan, D. J. Young and X. J. Loh, *Biomater Sci*, 2020, **8**, 776-797.
125.	T. Y. Kim, D. Y. Han and W. G. Lee, *Analytical Methods*, 2019, **11**, 1159-1167.
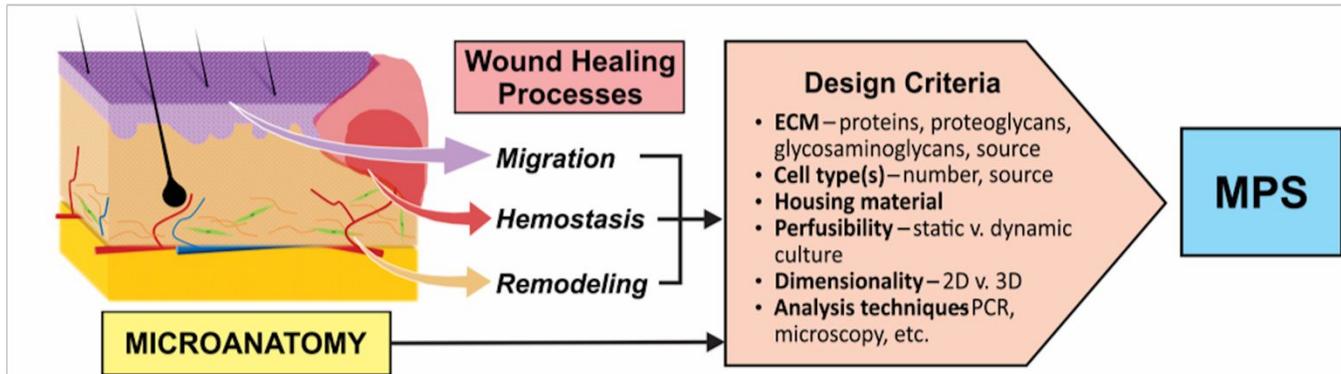
FIGURES

Figure 1. Design approaches and considerations for wound healing microphysiological systems. Common approaches for MPS design are to recreate a particular event or recreate a particular structure. Material and structural considerations are present in each approach. Migratory assays typically include epithelial cells, hemostasis assay typically include blood cells and/or vessel cells, and remodeling assays typically include fibroblasts and a 3D gel.
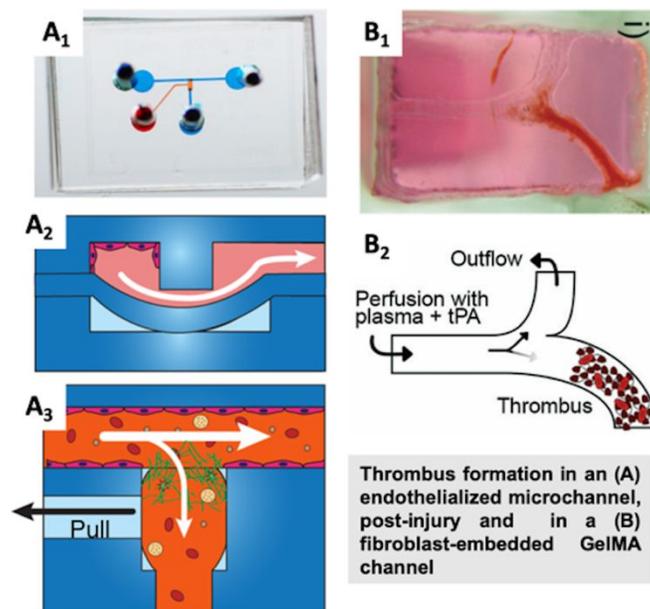
Figure 2. Hemostasis MPS. **A)** An endothelialized microchannel with a pressure-actuated valve for endothelial vessel damaging. Cellularized channels are 50µm x 150µm. **B)** A fibroblast-GelMA channel with or without endothelial cells allows visualization of thrombosis and observation of fibroblast migration. Channels are approximately 1–2mm wide. (A) and (B) reproduced with permission from ref 40: Copyright (2018) Nature Communications and ref 43: Copyright (2016) Royal Society of Chemistry, respectively.
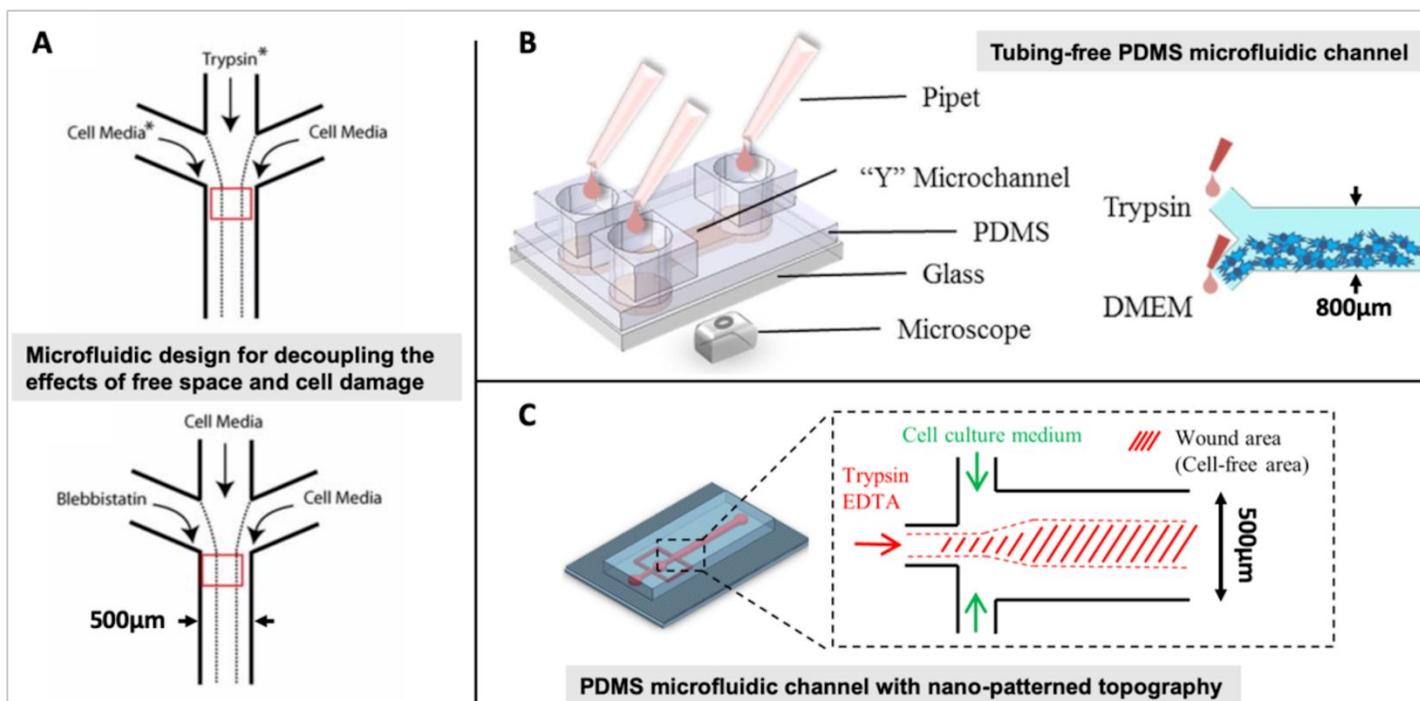
Figure 3. Microfluidic migration assay constructs. Laminar flow allows perfusions over defined regions of cell sheets. **A)** Comparison of migration tendencies due to free space or cell damage (perfusions of trypsin, ROS, or cell lysate), and the mediation of migration by tension (perfusions of blebbistatin, a contractility inhibitor). **C)** Nano-patterns introduce the effects of topography on cell migration. (A) – (C) reproduced with permission from ref 6: Copyright (2011) Murrell et al., ref 51: Copyright (2015) Nature, and ref 7: Copyright (2018) Lee et al., respectively.
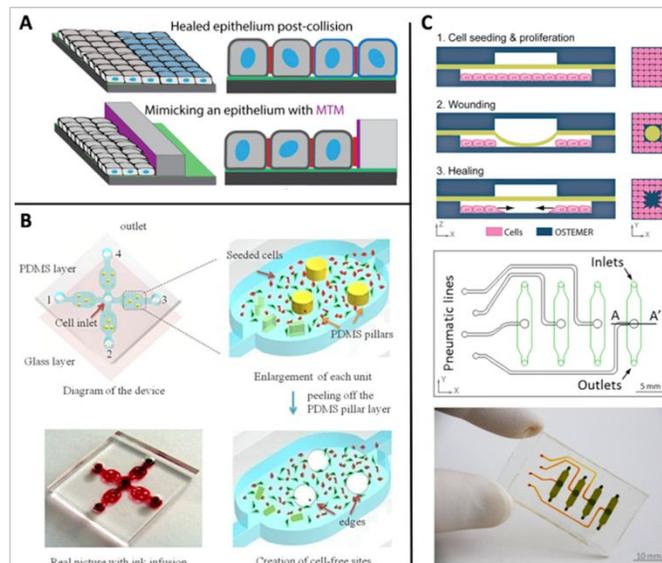
Figure 4. Barrier-based migration assay constructs. (**A**) Lateral presentation of E-cadherin (purple, red) recapitulates cell-cell recognition to halt migration and induce apical-basal polarity. (**B**) Multiple barriers in a single device allow high throughput analysis on glass. Pillar diameters are 800µm. (**C**) Pneumatic actuation of a PDMS membrane allows repeatable wounding in a defined area without disturbing ECM coatings. (A) – (C) reproduced with permission from ref 50: Proceedings of the National Academy of Sciences, ref 52: Copyright (2013) Wound Healing Society, and ref 54: Copyright (2017) American Chemical Society, respectively.
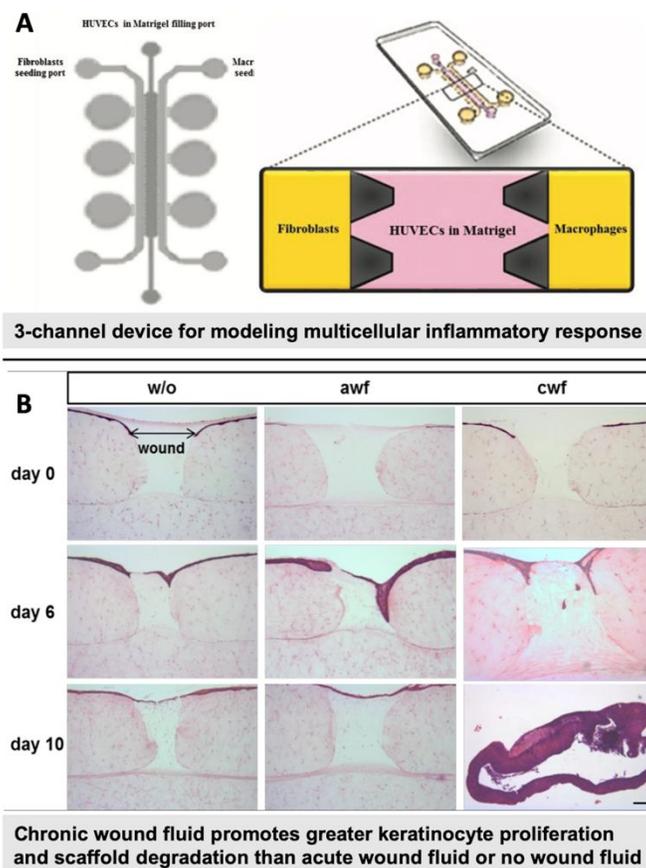
Figure 5. Remodeling assay constructs. **A)** Device for analyzing the influence of macrophages and/or fibroblasts on angiogenesis by HUVECs and the migratory tendency of fibroblasts. **B)** Addition of wound fluids to a skin construct demonstrates the imbalance of proliferation and degradation. (A) and (B) reproduced with permission from ref 74: Copyright (2018) Wiley Online Library and ref 75: Copyright (2017) Besser Manuela, et al., respectively.
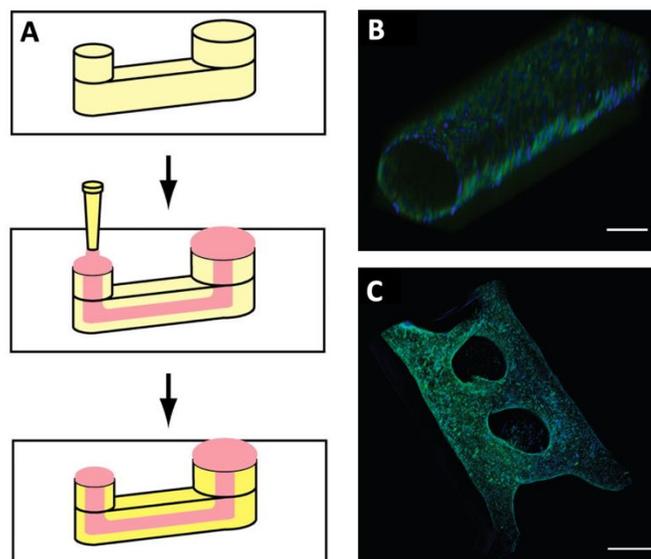
Figure 6. Viscous Finger Patterning. **A)** Passive pumping technique for the on-chip fabrication of lumen. Channels are first filled with an unpolymerized gel; less viscous cell media is then passively pumped through the gel and the gel is then polymerized. **B, C)** Confocal images of single (B) and multi-lumen (C) constructs with endothelial cells. Scale bars are 100μm (B) and 500μm (C). (A) – (C) reproduced with permission from ref 100: Copyright (2013) Elsevier.
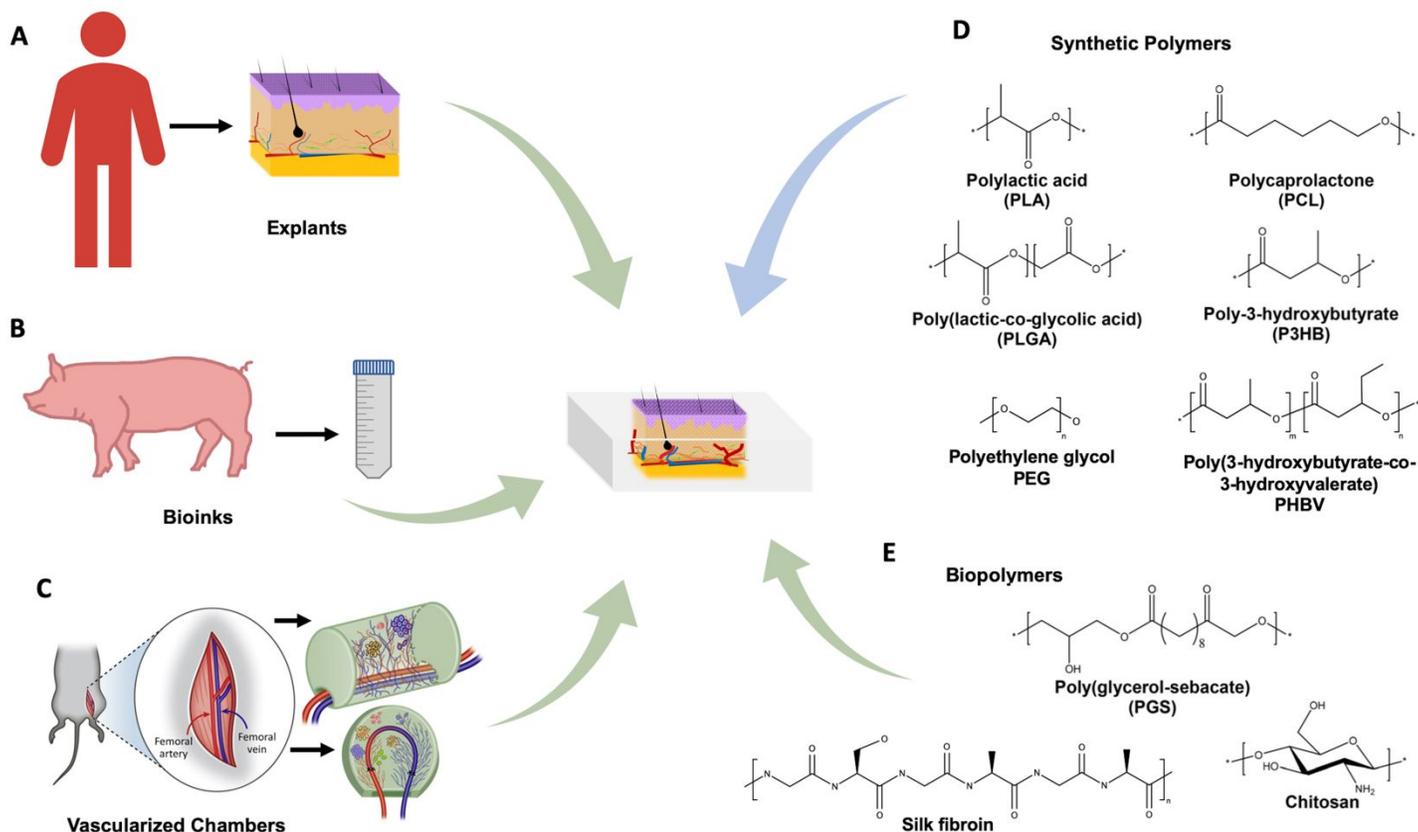
Figure 7. Summary of materials options in the fabrication of tissues within skin on chips. The colored arrows can be considered specific fabrication techniques, like bioprinting, viscous finger patterning, or electrospinning. **(A–E)** can overlap, e.g. PEG is a popular additive to natural hydrogels. **(D & E)**. Popular polymer choices in skin tissue engineering. Polysaccharides beyond chitosan include hyaluronic acid, agar, alginate, cellulose, and chitin. (C) Reproduced with permission from ref 106: Copyright (2018) Elsevier. Parts of (D) and (E) reproduced with permission from ref [124]: Copyright (2020) Royal Society of Chemistry.

TABLES

Table 1. Devices, materials, and fabrication techniques of wound healing devices by phase

WH Event	Cell Types	Materials	Fabrication Techniques	Ref.
Hemostasis	HUVECs, HAECs, platelets, RBCs	PDMS, collagen I or fibronectin coating	Soft lithography	[40]
	HUVECs, platelets, RBCs	PDMS, fibronectin/laminin coatings	Soft lithography	[42]
	HUVECs, HDFs, RBCs, platelets	PEG-GelMA, Pluronic F-127 (sacrificial)	Sacrificial bioprinting	[43]
	Platelets, RBCs	PDMS, collagen I and/or TF coatings, BSA coating	Soft lithography	[41]
	BOECs (porcine or human), HUVECs	PDMS, collagen I coating	Soft lithography	[44]
Migration	NIH-3T3s	PDMS, fibronectin coating	Capillary force lithography, soft lithography	[7]
	VSMCs	PDMS, collagen I or fibronectin coatings	Soft lithography	[51]
	CLS-1	Housing material not listed, fibronectin coating	photolithography	[6]
	GSE-1s, MSCs, ACCMs	Glass, PDMS	Soft lithography	[52]
	HUVECs	PDMS, OSTEMER, gelatin coating	Thermosetting, soft lithography	[54]
	MDCK	Fibronectin coated glass, E-cadherin-coated PDMS	Soft lithography	[50]
	HDFns	Fibrin gel, pNIPAm particles	Hydrogel in well plate	[63, 64]
	Skin explant, neutrophils	PDMS, full-thickness micro-biopsy	Soft lithography	[65]
	HeLa, TFC	Petri dish, PDMS	Soft lithography	[125]
Remodeling	HDFs, HaCaT	Collagen I gel, chronic and acute wound fluids	Hydrogel in well plate	[75]
	DFUFs, DFFs, NFFs, NHKs	Collagen I gel	——	[76]
	Rat heart fibroblasts	Fibrin gel, PDMS	Soft lithography	[72]
	M1/M2 macrophages, HDFs, HUVECs	Matrigel, PDMS	Soft lithography	[74]